ELSEVIER

SCIENCE DIRECT®

Physics Letters B 579 (2004) 251–257

PHYSICS LETTERS B

www.elsevier.com/locate/physletb

High-resolution determination of GT strength distributions relevant to the presupernova evolution using the $(d,{}^2\mathrm{He})$ reaction

M. Hagemann [a,1], A.M. van den Berg [b], D. De Frenne [a], V.M. Hannen [b,2], M.N. Harakeh [b], J. Heyse [a,3], M.A. de Huu [b], E. Jacobs [a], K. Langanke [c], G. Martínez-Pinedo [d,e,f], H.J. Wörtche [b]

[a] *Vakgroep Subatomaire en Stralingsfysica, Universiteit Gent, B-9000 Gent, Belgium*
[b] *Kernfysisch Versneller Instituut, NL-9747 AA Groningen, The Netherlands*
[c] *Institut for Fysik og Astronomi, Århus Universitet, DK-8000 Århus, Denmark*
[d] *Institut für Physik, Universität Basel, CH-4056 Basel, Switzerland*
[e] *Institució Catalana de Recerca i Estudis Avançats, Lluís Companys 23, E-08010 Barcelona, Spain*
[f] *Institut d'Estudis Espacials de Catalunya, Edifici Nexus, Gran Capità 2, E-08034 Barcelona, Spain*

Received 24 June 2003; received in revised form 29 August 2003; accepted 9 September 2003

Editor: V. Metag

Abstract

Spin–isospin excitations of the medium-mass nucleus ^{58}Co were studied using the (n,p)-type $(d,{}^2\mathrm{He})$ charge-exchange reaction at an incident energy $E_d = 170$ MeV and small scattering angles. The achieved energy resolution of 130 keV, full width at half maximum, allowed the extraction of Gamow–Teller strength to 13 peaks at excitation energies lower than 4.1 MeV in the residual nucleus ^{58}Co and is consistent with the results of a multipole-decomposition analysis. The identification of Gamow–Teller transitions is possible by comparison of the measured cross sections with DWBA calculations. The results are used to discuss the relevance of the Gamow–Teller strength distribution at low excitation energy with regard to electron-capture rates used in calculations for the final stage of a massive star.

PACS: 26.50.+x; 25.45.Kk; 27.40.+z; 25.45.-z

It was recognized by Bethe et al. [1] and by Fuller, Fowler and Newman (FFN) [2] that Gamow–Teller (GT) transitions in fp-shell nuclei play a decisive role in the calculation of the weak-interaction rates of processes taking place during the last few days of a heavy star in its presupernova stage. In recent years, new developments in nuclear-structure physics have led to renewed interest in the role of the GT strength distribution in fp-shell nuclei. The GT strength distribution can be determined using the $(d,{}^2\mathrm{He})$ reaction [3,4]. High-resolution spectra for this reaction are now available for light nuclei [5] and this program is be-

E-mail address: berg@kvi.nl (A.M. van den Berg).
[1] Present address: Robert Bosch GmbH, D-71229 Leonberg, Germany.
[2] Present address: SRON, NL-3584 CA Utrecht, The Netherlands.
[3] Present address: IRMM, Joint Research Centre, B-2440 Geel, Belgium.

0370-2693
doi:10.1016/j.physletb.2003.09.101

ing extended to medium-weight nuclei. From the theoretical side, the development of shell-model codes by Caurier et al. [6,7] and new computer hardware made it possible to calculate relevant strength distributions in fp-shell nuclei using about 10 million configurations. The results obtained in these recent large-scale shell-model calculations indicate that the electron-capture rates are generally smaller than was assumed by FFN [8]. These conclusions have led to a revision of presupernova models [9,10] resulting in a smaller mass of the iron core of the presupernova star and a larger value for the electron-to-baryon ratio Y_e as compared to the models based on the work of FFN.

Two things should be emphasized here. Firstly, because of phase-space considerations in the astrophysical environment, the electron-capture rates can depend strongly on the GT strength at low excitation energies. Secondly, the available experimental data obtained for the GT strength distribution have until recently been hampered by a rather poor energy resolution, making a detailed comparison between theory and experiment difficult. Nevertheless, the unpolarized (n, p) data obtained for fp-shell nuclei [11] have been used, amongst other data, as a benchmark for the recent large-scale shell-model calculations [7].

In this context, we report in this Letter on the results obtained for the ^{58}Ni$(d,^2\mathrm{He})$ charge-exchange reaction at a bombarding energy of 170 MeV. This reaction can be used to probe the GT strength distribution in the β^+ direction and to evaluate the impact on electron-capture rates in the astrophysical environment. The unbound di-proton system is referred to as ^{2}He, if the two protons are in a relative $^1S_0$ state. Experimentally, an almost pure $^1S_0$ state can be selected by limiting the relative energy of the di-proton system to less than 1 MeV, as in this case the contribution of higher-order partial waves is of the order of a few percent only [12]. Furthermore, the reaction mechanism forces a spin–flip and isospin–flip transition ($\Delta S = \Delta T = 1$). Therefore, at small momentum transfers, the $(d,^2\mathrm{He})$ reaction mainly probes the GT strength.

The ^{58}Ni$(d,^2\mathrm{He})$ reaction was studied at the AGOR facility at KVI using the Big-Bite Spectrometer [13] and the EuroSuperNova focal-plane detection system, which can be used amongst other things for the precise detection of ^{2}He at very small scattering angles [14]. A 170 MeV deuteron beam was used to bombard a 4.7 mg/cm^2 self-supporting ^{58}Ni target enriched to 99.8%. Using the dispersion-matching technique, an energy resolution of 130 keV full width at half maximum (fwhm) was achieved, which is at least a factor of 3 better than what has been achieved in former $(d,^2\mathrm{He})$ experiments [3,4,15]. The experimental method and data-reduction techniques have been described in our paper on the GT transitions to low-lying states in ^{12}B and ^{24}Na [5]. The extracted double-differential cross section up to $E_x = 10$ MeV is shown in Fig. 1(a) and compared to data from the ^{58}Ni(n, p) reaction [11]. Further details of the present analysis, together with a full description of the experimental procedure and analysis, will be presented in a forthcoming paper [16].

For the region $E_x < 4.1$ MeV, experimental angular distributions were obtained using the program FIT 3.0 [17] by fitting the spectra with peaks at 6 angular bins in the range between $\theta = 0^\circ$ and 6.5°. Up to $E_x = 2.3$ MeV, the excitation energy of $J^\pi = 1^+$ states listed in Ref. [18] were used in the fit. Between $2.3 < E_x < 4.1$ MeV, other peaks with $\Delta L = 0$ strength can be identified based on enhanced cross sections near a scattering angle of 0° as compared to more backward scattering angles (i.e., $\theta_{\mathrm{c.m.}} = 4^\circ$). The function used to fit all 13 peaks is a Gaussian with at both sides an additional exponential function used to describe the tails of the peaks. These tails are most likely caused by the reconstruction of the excitation energy in ^{58}Co from the measured momentum vectors of both protons detected in coincidence in the focal plane of the spectrometer. This reconstruction requires not only a determination of the energy of each proton but also its complete scattering angle at the object point (i.e., target position) of the spectrometer. In the applied fitting procedure the heights and positions of the peaks were varied, keeping their relative positions for all 6 angular bins fixed, while their widths were fixed to the measured resolution of 130 keV (fwhm). The relative positions for peaks 1 to and including 5 were taken from Ref. [18]. The relative positions of the other 8 peaks were taken from the comparison between forward and backward scattering angles. The parameters of the two additional exponential functions were chosen on basis of the fit of the peaks at low excitation energy; a detailed decomposition of these low-lying peaks is given in Fig. 1(b). As an exception a peak caused by contamination of the target with

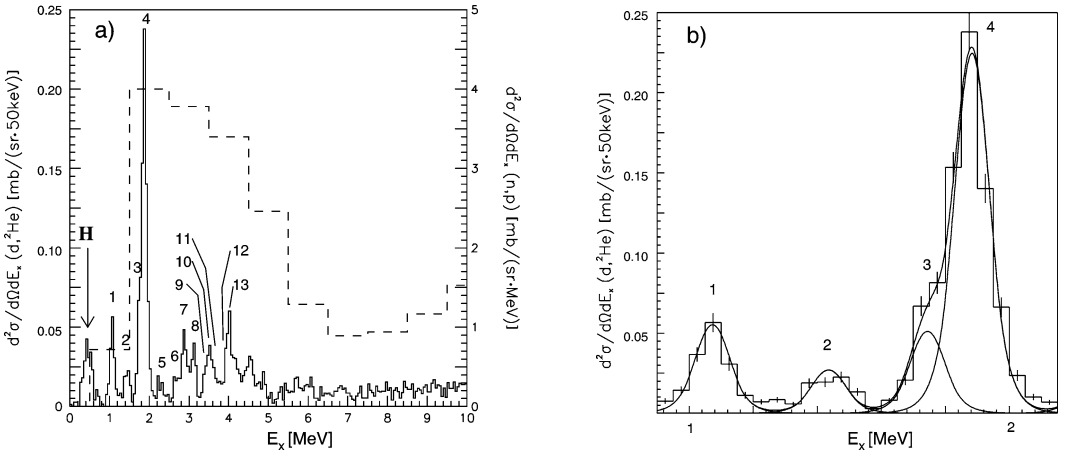

Fig. 1. (a) The solid histogram shows the double-differential cross section for the ^{58}Ni$(d,^2\mathrm{He})$ reaction integrated over the solid angle between $\theta = 0°$ and 1°. Numbers indicate peaks used in the data analysis (see Table 1). The peak caused by contamination of the target with hydrogen is indicated by 'H'. The dashed histogram presents the double-differential cross section from the (n, p) reaction at a scattering angle of $\theta = 0°$ measured by El-Kateb et al. [11]. (b) Fitted peaks for the $(d,^2\mathrm{He})$ spectrum at low excitation energy.

Table 1
Gamow–Teller strength for peaks identified in ^{58}Co using the ^{58}Ni$(d,^2\mathrm{He})$ reaction. The ratio $\sigma^{\Delta L=0}/\sigma^{\mathrm{tot}}$ denotes the $\Delta L = 0$ fraction of the cross section at 0.5°, neglecting the small D-state admixture in the wave function of the deuteron. The listed uncertainties are statistical only

	E_x in ^{58}Co (MeV)	$\frac{d\sigma^{\Delta L=0}(0.5°)}{d\Omega}$ (mb/sr)	$\sigma^{\Delta L=0}/\sigma^{\mathrm{tot}}$	$B_{\mathrm{exp}}(\mathrm{GT}^+)$
1	1.050[a]	0.159 ± 0.009	0.88[b]	0.15 ± 0.01
2	1.435[a]	0.078 ± 0.006	1.00	0.09 ± 0.01
3	1.729[a]	0.148 ± 0.014	1.00	0.16 ± 0.02
4	1.868[a]	0.648 ± 0.020	1.00	0.72 ± 0.05[c]
5	2.249[a]	0.047 ± 0.004	1.00	0.05 ± 0.01
6	2.66[d]	0.057 ± 0.005	0.96	0.06 ± 0.01
7	2.86[d]	0.145 ± 0.009	0.99	0.17 ± 0.01
8	3.10[d]	0.126 ± 0.008	0.99	0.15 ± 0.01
9	3.41[d]	0.065 ± 0.007	0.96	0.07 ± 0.01
10	3.52[d]	0.080 ± 0.009	0.95	0.09 ± 0.01
11	3.63[d]	0.067 ± 0.007	0.87	0.07 ± 0.01
12	3.90[d]	0.062 ± 0.006	0.97	0.07 ± 0.01
13	4.03[d]	0.155 ± 0.010	1.00	0.19 ± 0.01

[a] From Ref. [18].
[b] Mixture of $L = 0$ and $L = 2$; see Ref. [16].
[c] Normalized to Ref. [23] assuming isospin symmetry; see text.
[d] Estimated uncertainty is 25 keV.

hydrogen was fitted with a Gaussian-shaped peak of variable width, because of the kinematical broadening of this line. We estimate the uncertainty on the fitted excitation energies of the states 6 until 13 to be about 25 keV.

In Table 1, the identified $\Delta L = 0$ strength for $E_x < 4.1$ is summarized; it should be emphasized that for each peak listed, its angular distribution is consistent with an $L = 0$ transition as calculated in DWBA explained below. Although Ref. [18] lists for the region $2.3 < E_x < 4.1$ MeV many states with low spin values or even with tentative $J^\pi = 1^+$ assignments, a level-by-level comparison with our data set is very difficult. Because of this difficulty a multipole-decomposition analysis (MDA) has been made in addition to this peak-fitting procedure. In the MDA no explicit assumptions as to the shape or position of the contributing peaks or structures are made. For statistical rea-

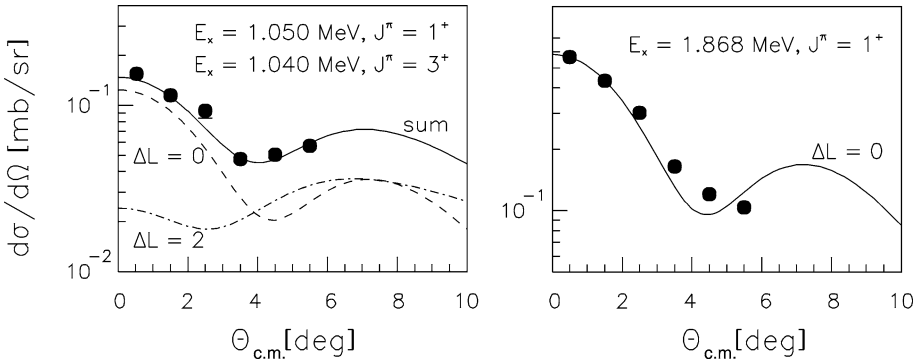

Fig. 2. Examples of differential cross sections observed in the ^{58}Ni$(d,^2\mathrm{He})$ reaction. The contributions from $\Delta L = 0, 2$ are indicated by the dashed, and the dash-dotted lines, respectively. The full line represents the incoherent sum of the components.

sons, the experimental excitation energy for the 6 different angular regions are binned into energy intervals of 1 MeV. Also no quasi-free charge-exchange background has been subtracted, following the assumption that the observed cross sections for $E_x < 7$ MeV are primarily originating from single-step reactions leading to 1p–1h excitations (see, e.g., Refs. [19,20]). The only input in the MDA is therefore the shape of the different angular distributions as a function of excitation energy and scattering angle.

The angular distributions for the $(d,^2\mathrm{He})$ reaction were calculated with the computer code ACCBA [21] in the distorted-wave Born approximation (DWBA). As an example, measured and calculated angular distributions for the excitation of two states are shown in Fig. 2. These calculated angular distributions and the deduced cross sections for the 6 angular bins were used to determine the cross section at $\theta_{\mathrm{c.m.}} = 0.5°$ for the 13 peaks identified in Fig. 1; see Table 1 for the results. In the MDA it is assumed that the measured differential cross sections can be written as an incoherent sum of the calculated cross sections weighted with coefficients $c_{\Delta J^\pi}$:

$$\sigma_{\mathrm{exp}}(\theta_{\mathrm{c.m.}}, E_x) = \sum_{\Delta J^\pi} c_{\Delta J^\pi} \times \sigma_{\mathrm{calc}}\big(\Delta J^\pi, \theta_{\mathrm{c.m.}}, E_x\big). \tag{1}$$

In principle, the sum should run over all allowed spin–parity transfers. However, microscopic calculations show that for small momentum transfers the shapes of the calculated angular distributions are predominantly characterized by the orbital angular momentum transfer ΔL. In the MDA the following transitions were taken into account $\Delta L = 0$, 1, and 2. Using a least-squares minimization procedure, the $\Delta L = 0$ cross sections at 0.5° have been extracted in this MDA and will be used to compare the GT strength distribution obtained through the peak-fitting procedure with the one based on the MDA. The measured $(d,^2\mathrm{He})$ cross sections $\sigma(q,\omega)$ for low momentum transfer $\Delta L = 0$, $J^\pi = 1^+$ transitions can be related to the corresponding GT strength $B(\mathrm{GT}^+)$ in a similar way as described by Taddeucci et al. [22] for the (p,n) reaction through:

$$B_{\mathrm{exp}}\big(\mathrm{GT}^+\big) = \frac{d\sigma(q=0,\omega=0)}{d\Omega}\left[\frac{d\hat{\sigma}_{\mathrm{GT}}}{d\Omega}\right]^{-1}, \tag{2}$$

where the proportionality factor $\hat{\sigma}_{\mathrm{GT}}$ is called the "unit cross section". In all cases, the cross section at zero momentum transfer and zero energy transfer can be related to the experimental cross section measured at small scattering angles using an extrapolation based on DWBA:

$$\frac{d\sigma(q=0,\omega=0)}{d\Omega} = \frac{d\sigma_{\mathrm{exp}}(q,\omega)}{d\Omega} \times \frac{\sigma_{\mathrm{DWBA}}(q=0,\omega=0)}{\sigma_{\mathrm{DWBA}}(q,\omega)}. \tag{3}$$

Because we have made our measurement at small scattering angles, this correction is for excitation energies up to 10 MeV less than 15%. The unit cross section $\hat{\sigma}_{\mathrm{GT}}$ was evaluated by comparing the strongest peak in the $(d,^2\mathrm{He})$ spectrum at 1.868 MeV with its isobaric analog transition measured in the $(^3\mathrm{He},t)$ reaction at 450 MeV. The ^{58}Ni$(^3\mathrm{He},t)$ reaction revealed a $B_{\mathrm{exp}}(\mathrm{GT}^-)$ value of 0.120 ± 0.008 for the analog peak at 10.82 MeV in ^{58}Cu [23]. Applying isospin symmetry for the $A = 58$ system [24], the squares of the

isospin Clebsch–Gordan coefficients for the (p,n)-type and the (n,p)-type reactions on ^{58}Ni, for which the isospin quantum numbers of its ground state are $T = T_z = 1$, can be calculated to be $1/6$ and 1, respectively. Thus, the GT^+ strength of the analog transition in the $(d,^2\mathrm{He})$ reaction to the state at 1.868 MeV in ^{58}Co can be assigned to be 0.72 ± 0.05. The unresolved peak to left of peak number 4 is the 1.729 MeV $J^\pi = 1^+$ state listed in Ref. [18]. It should be noted that in the work of Ref. [23] a $J^\pi = 1^+$ state at 10.597 MeV in ^{58}Cu and at 10.492 MeV in ^{58}Ni was identified through the $(^3\mathrm{He},t)$ and (p,p') reactions, respectively. Again using isospin symmetry these states may very well correspond to the known 1.729 MeV state in ^{58}Co which is further supported by the value of the $B(GT^-)$ strength measured in the $(^3\mathrm{He},t)$ reaction: $B(GT^-) = 0.028 \pm 0.006$ [23]. This should correspond to 0.17 ± 0.04 for the $(d,^2\mathrm{He})$ reaction, in agreement with our data: $B_{\mathrm{exp}}(GT) = 0.16 \pm 0.02$. Using Eq. (2), the differential unit cross section for the transition to peak number 4 shown in Fig. 1 can be calculated to be $d\hat{\sigma}_{GT}/d\Omega = 1.01 \pm 0.06$ mb/sr. In all cases, the $B_{\mathrm{exp}}(GT)$ values are given in such units that for the β-decay of the free neutron, $B_{\mathrm{exp}}(GT) = 3$. In Table 1 the results of the analysis based on the peak-fitting procedure are summarized. Transitions to known 1^+ states were assumed to be pure GT^+ transitions, whereas for other transitions the result of the fitting procedure was used to extract their $\Delta L = 0$ contribution; see Ref. [16] for details. In Table 2, the results of the MDA are listed. In both tables, the indicated errors for the cross sections and the $B_{\mathrm{exp}}(GT^+)$ values are statistical only. We estimate the systematic error on the $(d,^2\mathrm{He})$ cross sections, which includes also the acceptance correction of the spectrometer [14, 16], to be about 20%.

In Fig. 3, we compare the $B(GT^+)$ strength obtained from the present experiment, with the data from the (n,p) reaction [11]. The dots in the upper panel represent the results from the peak-fitting procedure; the gray histogram those from the MDA. Up to an excitation energy of 4 MeV, the integrated $B_{\mathrm{exp}}(GT^+)$ strength obtained through the two different methods is consistent: 2.04 ± 0.06 for the peak-fitting procedure versus 1.9 ± 0.2 for the MDA. Taking into account systematic errors, we find up to $E_x = 4$ MeV an integrated $B(GT^+)$ value of 2.1 ± 0.4, which is in agreement with the integrated $B(GT^+)$ strength of 2.7 ± 0.3 deduced from the (n,p) reaction [11]. In the lower panel of Fig. 3, we present the results of large-scale shell-model calculations for the GT strength distribution. The open squares show the results of the calculations performed by Caurier et al. [7] which have been used in the tabulation of weak-interaction rates [8]. The results displayed as dots have been obtained us-

Table 2
Gamow–Teller strength identified in ^{58}Co using MDA

E_x in ^{58}Co (MeV)	$B_{\mathrm{exp}}(GT^+)$
0.5	0.06 ± 0.05
1.5	0.97 ± 0.12
2.5	0.34 ± 0.06
3.5	0.53 ± 0.07
4.5	0.48 ± 0.07
5.5	0.23 ± 0.04
6.5	0.19 ± 0.04
7.5	0.17 ± 0.03
8.5	0.20 ± 0.04
9.5	0.23 ± 0.04

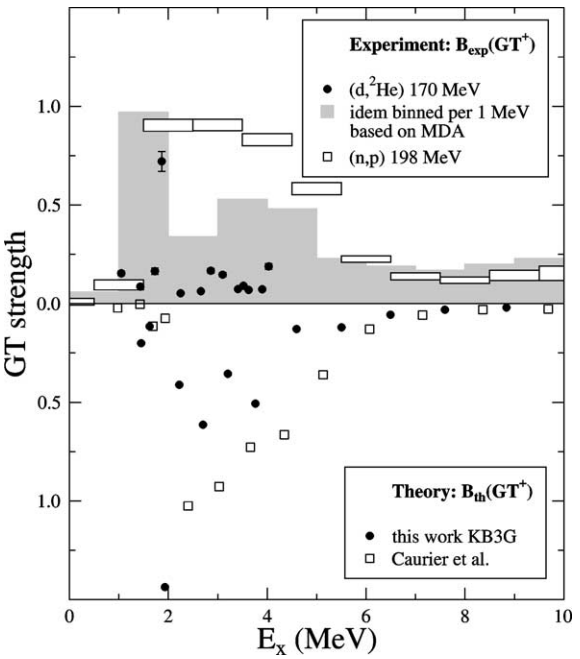

Fig. 3. Upper panel: the experimental GT strength distribution listed per peak (dots; see Table 1) and per bin of 1 MeV (gray histogram; see Table 2). In addition, we show the results from the (n,p) reaction [11] in GT strength per MeV. Lower panel: the results from the present calculations using the KB3G interaction and those from Caurier et al. [7].

ing the more recent KB3G effective interaction [25]. It should be noted that the theoretical results have been calculated using a quenching factor of 0.74 for the GT operator (cf. Ref. [25]). It is seen from this figure, that the new calculations using the KB3G interaction reproduce the GT strength distribution as obtained from the $(d,^2\mathrm{He})$ reaction fairly well, especially for the low-lying states; this is in contrast to the results from the earlier calculations [7].

The experimental data will now be used to see if these new results can have an impact on the electron-capture rate in the stellar environment. The method to calculate electron-capture rates follows the formalism derived by FFN [2]. As representative values for the temperature, density and Y_e we take the conditions following silicon depletion for the model labeled LMP listed in Table 2 of Ref. [10] ($T_9 = 4.05$ where T_9 measures temperatures in units of 10^9 K, $\rho = 3.18 \times 10^7\ \mathrm{g\,cm^{-3}}$, $Y_e = 0.48$). This corresponds to the evolution of the core of a 25 $M_\odot$ star using the weak-interaction rates of Ref. [8]. At the finite temperature conditions present in the star, the contribution of transitions starting from excited nuclear states is non-negligible. For the particular conditions given above, the shell-model calculations predict that the contribution of excited states of ^{58}Ni enhances by 50% the rate as calculated using only the ground-state contribution. Therefore, we keep the contribution of excited states fixed as determined by the calculations of Ref. [8] and recompute the ground-state contribution using the GT-strength distribution measured in the (n, p) and $(d,^2\mathrm{He})$ reactions or computed using the KB3G interaction. Fig. 4 displays the rate as a function of temperature and for the values of density and Y_e discussed above. The theoretical rates computed in Ref. [8] and those based on the KB3G interaction use experimental excitation energies for the first two 1^+ states in ^{58}Co as given in Ref. [18]. It is seen from this figure that especially at low temperatures the details of the GT-strength distribution has a strong impact on the electron-capture rate. The rates calculated applying the results from the MDA (see Table 2) are substantially larger as compared to the rates using the high-resolution data listed in Table 1.

Fig. 5 shows the electron-capture rates relative to the ones computed using the $(d,^2\mathrm{He})$ data for the ground-state contribution as listed in Table 1. It is seen that the rate based on the KB3G interaction and on the

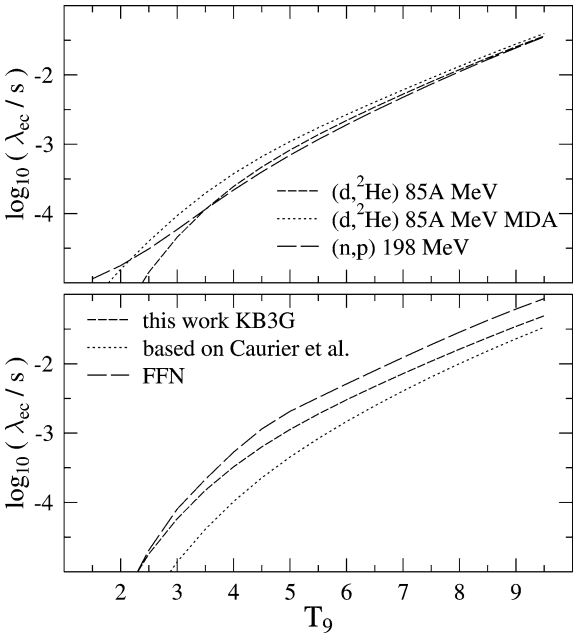

Fig. 4. Upper panel: electron-capture rates using GT strength from the (n, p) measurement [11], and the $(d,^2\mathrm{He})$ measurement with data as listed in Tables 1 and 2. Lower panel: obtained from the shell-model calculations using the KB3G interaction, the earlier work of FFN [2], and Caurier et al. [7].

(n, p) data agree rather well for the relevant temperature range ($3 < T_9 < 4$). The rate based on the calculations of Caurier et al. [7] shows deviations of a factor 3 and more for the lowest temperatures. However, this effect does not seem to be systematic as both the KB3G interaction and the interaction of Ref. [7] yield a similar description for the decay of ^{56}Cu [26]. For the relevant temperature range, the FFN rate deviates by at most a factor 2. It should be noted that this FFN rate [2] does not include any quenching factor which, if taken into account, will cause the rates to become smaller. It is clear from Fig. 5 that the new high-resolution experimental information can provide the clues to decide between otherwise rather similar effective interactions. Moreover, in the calculations the location of the states at low-lying excitation energy are constrained by experimental data, which is of course important at the lower temperatures. We note here that there are many nuclei which contribute, often more significantly than ^{58}Ni, to the electron-capture rate in the presupernova stage. It is therefore quite important to check the shell-model predictions for other

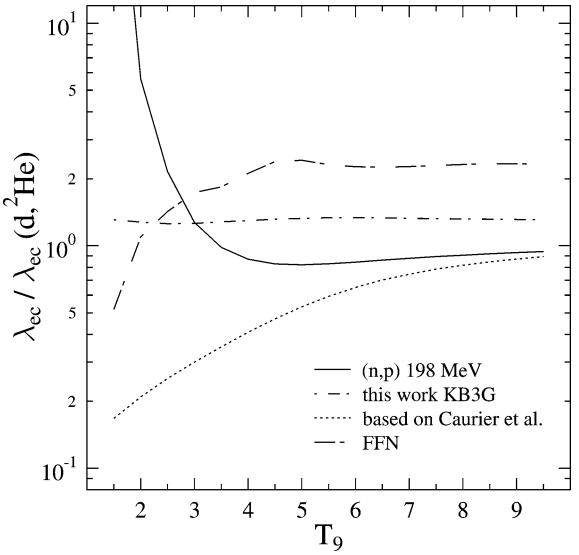

Fig. 5. Electron-capture rates relative to the rate obtained from the $(d,^2\mathrm{He})$ data; see also caption to Fig. 4.

nuclei. In particular, the noted difference between the FFN [2] and the large-scale shell-model calculation, calls for a crucial test of both calculations using the present technique employing the $(d,^2\mathrm{He})$ reaction. In addition, the use of radioactive-ion beams to study the GT strength distribution is of importance, especially for $(N-Z)/A > 0.1$, where the GT strength moves to even lower excitation energy [8]. For instance, ^{60}Co is a key nucleus because based on the FFN model, the most important electron-capture rate is caused by the $^{60}\mathrm{Co}(e^-,\nu)^{60}\mathrm{Fe}$ reaction [9] for a huge range of temperatures and densities during the presupernova evolution. This rate is greatly reduced in the tabulation of Ref. [8]. Future high-resolution data could provide an accurate determination of the electron-capture rate on ^{60}Co.

Acknowledgements

This work was performed as part of the research program of the Fund for Scientific Research—Flanders (Belgium), the research program of the *Stichting voor Fundamenteel Onderzoek der Materie (FOM)* with financial support from the *Nederlandse Organisatie voor Wetenschappelijk Onderzoek (NWO)*. Further financial support was obtained from the EC under contract number TMR-LSF-ERBFMGECT980125.

References

[1] H.A. Bethe, et al., Nucl. Phys. A 324 (1979) 487.
[2] G.M. Fuller, W.A. Fowler, M.J. Newman, Astrophys. J. Suppl. Ser. 42 (1980) 447;
G.M. Fuller, W.A. Fowler, M.J. Newman, Astrophys. J. Suppl. Ser. 48 (1982) 279;
G.M. Fuller, W.A. Fowler, M.J. Newman, Astrophys. J. 252 (1982) 715;
G.M. Fuller, W.A. Fowler, M.J. Newman, Astrophys. J. 293 (1985) 1.
[3] H. Ohnuma, et al., Phys. Rev. C 47 (1993) 648.
[4] H.M. Xu, et al., Phys. Rev. C 52 (1995) 1161.
[5] S. Rakers, et al., Phys. Rev. C 65 (2002) 044323.
[6] E. Caurier, Computer code ANTOINE, IReS Strasbourg, 1989; E. Caurier, F. Nowacki, Computer code NATHAN, IReS Strasbourg, 1998, unpublished.
[7] E. Caurier, et al., Nucl. Phys. A 653 (1999) 439.
[8] K. Langanke, G. Martínez-Pinedo, Nucl. Phys. A 673 (2000) 481;
K. Langanke, G. Martínez-Pinedo, At. Data Nucl. Data Tables 79 (2001) 1.
[9] A. Heger, K. Langanke, G. Martínez-Pinedo, S.E. Woosley, Phys. Rev. Lett. 86 (2001) 1678.
[10] A. Heger, S.E. Woosley, G. Martínez-Pinedo, K. Langanke, Astrophys. J. 560 (2001) 307.
[11] S. El-Kateb, et al., Phys. Rev. C 49 (1994) 3128.
[12] S. Kox, et al., Nucl. Phys. A 556 (1993) 621.
[13] A.M. van den Berg, Nucl. Instrum. Methods B 99 (1995) 637.
[14] S. Rakers, et al., Nucl. Instrum. Methods A 481 (2002) 253.
[15] H. Okamura, et al., Phys. Lett. B 345 (1995) 1.
[16] M. Hagemann, et al., in preparation.
[17] S. Strauch, F. Neumeyer, Computer code FIT 3.0, TU Darmstadt, 1996, unpublished.
[18] M.R. Bhat, Nucl. Data Sheets 80 (1997) 789.
[19] M.A. Moinester, Can. J. Phys. 65 (1987) 660.
[20] J. Jänecke, et al., Phys. Rev. C 48 (1993) 2828.
[21] H. Okamura, Phys. Rev. C 60 (1999) 064602.
[22] T.N. Taddeucci, et al., Nucl. Phys. A 469 (1987) 125.
[23] H. Fujita, Ph.D. thesis, Osaka University, Osaka, Japan, 2002, unpublished.
[24] Y. Fujita, et al., Phys. Lett. B 365 (1996) 29.
[25] A. Poves, J. Sánchez-Solano, E. Caurier, F. Nowacki, Nucl. Phys. A 694 (2001) 157.
[26] R. Borcea, et al., Nucl. Phys. A 695 (2001) 69.